CHIN. PHYS. LETT. Vol. 30, No. 9 (2013) 096103

Wake Effects in Ion Transport through Carbon Nanotubes *

ZHANG Ying-Ying(张莹莹), ZHAO Dan(赵丹), YOU Shu-Yan(尤术艳),
SONG Yuan-Hong(宋远红)**, WANG You-Nian(王友年)

School of Physics and Optoelectronic Technology, Dalian University of Technology, Dalian 116024

(Received 12 April 2013)

A semiclassical kinetic model is explored to investigate the wake effects in the transport of charged particles through single-walled (SWCNT) and double-walled (2WCNTs) carbon nanotubes, with the introduction of electron band structure effect. The analytical expressions of the induced electron density at nanotube surface and the induced potential around the nanotube walls are obtained. The simulation results indicate that a bell-like distribution appears for the induced electron density when the incident particle speed is below a threshold value, otherwise wake-like oscillation can be seen behind the particle in the axial distribution. Dependencies of the amplitude and frequency of oscillations on the incident particle speed are also discussed. Meanwhile, we notice that the valence electrons on the outer wall of 2WCNTs tend to be easily excited by the polarized electrons on the inner wall, compared with that by the incident particle without the inner wall in SWCNTs. Finally, the induced potential trailing the incident particle also exhibits remarkable oscillations, not only along the axial direction but also in the lateral region, with evident extrema at the nanotube walls.

PACS: 61.85.p 73.21.−b, 73.63.−b DOI: 10.1088/0256-307X/30/9/096103

Interaction of charged particles with carbon nanotubes has been the major subject of research in both theoretical and experimental aspects. With hollow structure and remarkable electronic properties, carbon nanotubes have been proposed for several potential applications, such as in semiconducting devices and biomedicine. In addition, the progressive technology of ordering and straightening of carbon nanotube arrays makes carbon nanotubes become a possible candidate for channeling applications. In particular, Zhu *et al.*[1] first reported the experimental results on 2 MeV He^+ ions channeling in carbon nanotubes. Then, the channeling of energetic electrons through single and multiwall carbon nanotubes were realized by Chai *et al.*[2] in experiments. More recently, the transport of small single-stranded DNA oligomers through carbon nanotubes[3] were discussed, which may open avenues for control of DNA translocation.

Meanwhile, achievements have been acquired in the theoretical investigation on the channeling charged particles through carbon nanotubes.[4−6] During the channeling, one of the most concerning problems is the response of valence electrons on carbon nanotubes, including the electron density of the nanotube surface and induced potential around the walls of nanotubes. Theoretical research on the wake effects on the interaction of fast ions with carbon nanotubes has been carried out by Mowbray *et al.*,[7] indicating that a threshold value of the charged particle speed exists in the oscillatory wake effects. In the framework of the dielectric-response theory, the properties of the induced density in doped graphene due to an external moving charged particle were investigated in Ref. [8]. The first experimental evidence for the existence of image-potential states in carbon nanotubes has been presented by Zamkov *et al.*[9]

In addition, it has been known from the corresponding research that, for high-energy (GeV)[10−13] and low-energy (keV)[14,15] particles, the effects of dynamic polarization of the valence electrons of nanotubes on the transport of particles are almost negligible, while for the particles with medium (keV–MeV) energy, the valence electrons of nanotube surface are inclined to respond to the projectile particles, owing to the matching of the ion speeds and those of the valence electrons in nanotubes.[16] Therefore, the dynamic polarization may play an important role in the interaction processes between intermediate energy ions and carbon nanotubes, which has been confirmed by Arista[17,18] in research of swift ions and molecules moving in cylindrical channels, micro-capillaries and nanotubes. In the existence of dynamic polarization, the ion trajectories oscillate over the peripheral radial region inside the carbon nanotubes, which is entirely different from the conditions without consideration of the dynamical polarization force.[19]

As we know, nanotubes can exhibit either metallic or semiconducting properties, associated with the rolling pattern of a planar sheet to a cylindrical cavity. Thus, dependent on the actual geometrical structure, the energy band structure of the electrons on the nanotube wall should be introduced in the theoretical investigation on the interaction of ions with nanotubes. A semiclassical kinetic model was proposed to describe the electromagnetic processes in carbon nanotubes for different band structures,[20] where the electron dispersion relation is in the framework of the tight-binding model.[21] By adopting this kinetic model combined with the dielectric response theory, we studied the collective excitation of the surface electrons during the transport of a charged particle in the zigzag and armchair nanotubes of metallic character in

*Supported by the National Natural Science Foundation of China under Grant No 10975028, the National Basic Research Program of China under Grant No 2010CB832901, and Program for New Century Excellent Talents in University NCET-08-0073.
**Corresponding author. Email: songyh@dlut.edu.cn
© 2013 Chinese Physical Society and IOP Publishing Ltd

our previous works.[22,23] Then, the theoretical model was extended to describe the electronic excitation in 2WCNTs.[24] The analytical expressions of the self-energy and stopping power were also obtained, which can manifest the local features of the induced potential where the ions are located.

In this Letter, the kinetic model will be extended to focus our particular attention on the wake effects of the induced electron density and induced potential, with charged particles moving in both SWCNTs and 2WCNTs of metallic character. The valence electrons are perturbed by the intruding particle, bringing about electron polarization. When carbon nanotubes are in equilibrium state, the valence electrons on the walls meet the Fermi equilibrium distribution.[20] In addition, π electrons are the only electrons we care about for their important effects on electronic properties. Atomic units (a.u.) will be used throughout this study.

Both SWCNT and 2WCNT are regarded as infinitely long and infinitesimally thin cylindrical shells. The SWCNT with radius a, and the 2WCNT consists of 2 coaxial walls with the inner radius a_1 and the outer radius a_2, respectively. We use the cylindrical coordinate system $r = (\rho, \phi, z)$ here, with the orientation of z parallel to the axis of nanotubes. Considering a charged particle Q tracking parallel to the axis of SWCNT or 2WCNT at constant speed v, we confirm that the particle instantaneous position is given by $r_0 = (\rho_0, \phi_0, vt)$, here $\rho_0 < a$ or $\rho_0 < a_1$.

For SWCNTs, we employ Φ_1^1 and Φ_2^1 to express the total potential inside ($\rho < a$) and outside ($\rho > a$) the nanotube, while the value of the inside potential can be expressed as $\Phi_1^1 = \Phi_0^1 + \Phi_{\rm ind}^1$. The induced potential $\Phi_{\rm ind}^1$ is caused by the charge polarization on the nanotube surface and the potential Φ_0^1 represents the Coulomb potential from the moving charged particle itself, which could be expanded in terms of cylindrical Bessel functions $I_m(x)$ and $K_m(x)$. According to the work of Ref. [23], the induced potential $\Phi_{\rm ind}^1$ and Φ_2^1 can be given as follows

$$\begin{aligned}\Phi_{\rm ind}^1 = &\frac{Q}{\pi}\sum_{m=-\infty}^{\infty}\int_{-\infty}^{\infty} dk e^{ik(z-vt)+im(\phi-\phi_0)}\\ &\cdot I_m(|k|\rho_0)I_m(|k|\rho)\\ &\cdot \frac{K_m(|k|a)}{I_m(|k|a)}[\epsilon^{-1}(k,m,\omega,a)-1],\\ &\qquad \text{for } \rho < a, \end{aligned} \tag{1}$$

$$\begin{aligned}\Phi_2^1 = &\frac{Q}{\pi}\sum_{m=-\infty}^{\infty}\int_{-\infty}^{\infty} dk e^{ik(z-vt)+im(\phi-\phi_0)}\\ &\cdot I_m(|k|\rho_0)K_m(|k|\rho)\\ &\cdot \epsilon^{-1}(k,m,\omega,a), \qquad \text{for } \rho > a, \end{aligned} \tag{2}$$

where k is the wave number along the axial direction denoted by z; m is the angular momentum; $\epsilon(k,m,\omega,a)$ is the dielectric function of the electron gas on the nanotube surface with the form $\epsilon(k,m,\omega,a) = 1 - 4\pi a I_m(ka)K_m(ka)\chi(k,m,\omega,a)$; $\chi(k,m,\omega,a)$[22] of the last term is the response function of the carbon nanotubes with different expressions for zigzag and armchair nanotubes owing to the distinctive energy band structure, with ω being the frequency of the elementary excitation. The induced electron density n^1 on the surface of the nanotubes is obtained as follows:

$$\begin{aligned} n^1 = -\frac{Q}{\pi}&\sum_{m=-\infty}^{\infty}\int_{-\infty}^{\infty} dk e^{ik(z-vt)+im(\phi-\phi_0)}\\ &\cdot I_m(|k|\rho_0)K_m(|k|a)\\ &\cdot \epsilon^{-1}(k,m,\omega,a)\chi(k,m,\omega,a). \end{aligned} \tag{3}$$

Similarly, for 2WCNTs, we employ Φ_1^2, Φ_2^2 and Φ_3^2 to express the total potential inside the inner wall ($\rho < a_1$), the potential between two walls ($a_1 < \rho < a_2$), and the potential outside the outer wall ($a_2 < \rho$), respectively. The potential $\Phi_1^2 = \Phi_0^2 + \Phi_{\rm ind}^2$ is analogous to Φ_1^1. Based on the previous work,[24] these potentials can be given by

$$\begin{aligned}\Phi_{\rm ind}^2 = &\frac{Q}{\pi}\sum_{m=-\infty}^{\infty}\int_{-\infty}^{\infty} dk e^{ik(z-vt)+im(\phi-\phi_0)}\\ &\cdot I_m(|k|\rho_0)I_m(|k|\rho)\\ &\cdot \frac{K_m(|k|a_1)}{I_m(|k|a_1)}\Big\{\epsilon^{-1}(k,m,\omega,a_j)[1-4\pi a_2\\ &\cdot I_m(|k|a_2)K_m(|k|a_2)\chi(k,m,\omega,a_2)\\ &+\frac{4\pi a_2 K_m^2(|k|a_2)I_m(|k|a_1)}{K_m(|k|a_1)}\\ &\cdot \chi(k,m,\omega,a_2)]-1\Big\}, \qquad \text{for } \rho < a_1, \end{aligned} \tag{4}$$

$$\begin{aligned}\Phi_2^2 = &\frac{Q}{\pi}\sum_{m=-\infty}^{\infty}\int_{-\infty}^{\infty} dk e^{ik(z-vt)+im(\phi-\phi_0)}I_m(|k|\rho_0)\\ &\cdot \epsilon^{-1}(k,m,\omega,a_j)\big\{[1-4\pi a_2\\ &\cdot I_m(|k|a_2)K_m(|k|a_2)\chi(k,m,\omega,a_2)]\\ &\cdot K_m(|k|\rho)+4\pi a_2 K_m^2(|k|a_2)\chi(k,m,\omega,a_2)\\ &\cdot I_m(|k|\rho)\big\}, \qquad \text{for } a_1 < \rho < a_2, \end{aligned} \tag{5}$$

$$\begin{aligned}\Phi_3^2 = &\frac{Q}{\pi}\sum_{m=-\infty}^{\infty}\int_{-\infty}^{\infty} dk e^{ik(z-vt)+im(\phi-\phi_0)}I_m(|k|\rho_0)\\ &\cdot K_m(|k|\rho)\epsilon^{-1}(k,m,\omega,a_j), \qquad \text{for } \rho > a_2, \end{aligned} \tag{6}$$

where $j = 1, 2$ and

$$\begin{aligned}\epsilon(k,m,\omega,a_j) = &[1-4\pi a_1 I_m(|k|a_1)K_m(|k|a_1)\\ &\cdot \chi(k,m,\omega,a_1)]\\ &\cdot [1-4\pi a_2 I_m(|k|a_2)K_m(|k|a_2)\\ &\cdot \chi(k,m,\omega,a_2)]\\ &-[4\pi I_m(|k|a_1)K_m(|k|a_2)]^2 a_1 a_2\\ &\cdot \chi(k,m,\omega,a_1)\chi(k,m,\omega,a_2). \end{aligned}$$

Then the induced electron density n_j^2 is obtained as follows:

$$
\begin{aligned}
n_j^2 = \frac{Q}{\pi} \sum_{m=-\infty}^{\infty} \int_{-\infty}^{\infty} dk e^{ik(z-vt)+im(\phi-\phi_0)} I_m(|k|\rho_0) \\
\cdot \epsilon^{-1}(k,m,\omega,a_j)\chi(k,m,\omega,a_j) \\
\cdot \big\{[1-4\pi a_2\ I_m(|k|a_2)K_m(|k|a_2)\chi(k,m,\omega,a_2)] \\
\cdot K_m(|k|a_j) + 4\pi a_2 K_m^2(|k|a_2)\chi(k,m,\omega,a_2) \\
\cdot I_m(|k|a_j)\big\}, \qquad j=(1,2). \qquad (7)
\end{aligned}
$$

In the following calculations, we consider the charged particle as a proton ($Q = 1$) tracking along the axis ($\rho_0 = 0$) of SWCNT or 2WCNT. The friction coefficient is set at $\gamma = 0.001\omega_p$, with the classical plasma frequency in homogeneous electron gas $\omega_p = (\frac{4\pi n_0}{a})^{\frac{1}{2}}$. Here n_0 is the surface density of the valence electrons. In addition, for the case of axial symmetry, only $m = 0$ can be relied on in the investigation.

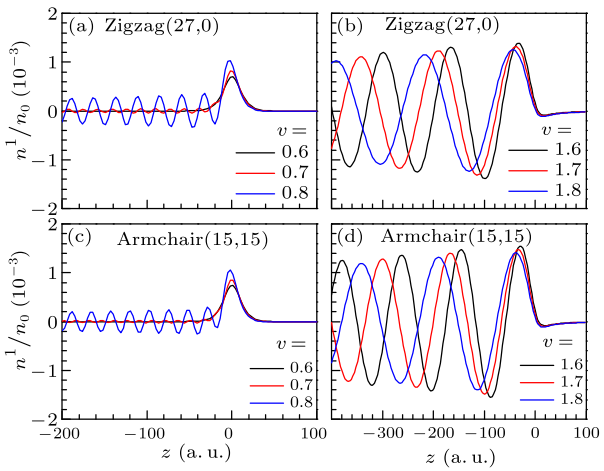

Fig. 1. The rate of the induced electron density $\frac{n^1}{n_0}$ dependent on the axial position z in the plane $\phi = \phi_0$, as the proton moves along the axis of zigzag (27,0) and armchair (15,15) SWCNT respectively, at lower speeds $v = 0.6, 0.7, 0.8$ a.u. in (a) and (c), or higher speeds $v = 1.6, 1.7, 1.8$ a.u. in (b) and (d).

Figure 1 shows the SWCNT induced electron density ratio $\frac{n^1}{n_0}$ versus the axial position z in the plane $\phi = \phi_0$, for zigzag (27,0) nanotube with radius $a = 20.25$ a.u. and armchair (15,15) nanotube with $a = 20.79$ a.u. It can be seen that there exists a threshold value for the proton speed about $v = 0.7$ a.u. from Figs. 1(a) and 1(c). When the projectile proton's speed is below the threshold value, the induced electron density exhibits a bell-like distribution, similar to the work in Ref. [7], while above the threshold value, wake-like oscillations can be observed in the axial distribution for both metallic nanotubes, as shown in Figs. 1(b) and 1(d). According to Ref. [8], the collective excitation, i.e. the usual wake oscillations, can occur only when the particle speed matches the phase velocity of the plasmons of CNTs, because of the Landau damping. Furthermore, making a comparison from Figs. 1(a) and 1(b), 1(c) and 1(d), we can obtain that as the particle speed increases, the amplitude of oscillations increases in magnitude when trailing at lower speeds, but decreases in the higher speed range. Meanwhile, the frequency of oscillations keeps decreasing with the increasing particle speeds. Furthermore, it can also be noticed that the positions of the first peak of trailing oscillations shift to the opposite direction of the z axis as the speed increases, for all the induced electron density curves at lower speeds as well as higher speeds.

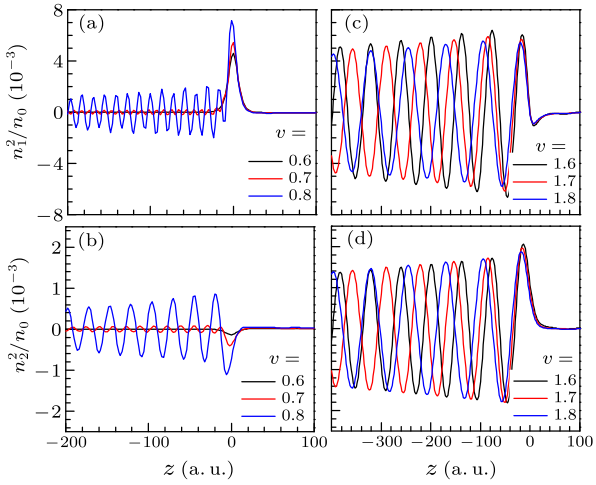

Fig. 2. The rate of the inner $\frac{n_1^2}{n_0}$ and outer $\frac{n_2^2}{n_0}$ induced electron densities dependent on the axial position z in the plane $\phi = \phi_0$, as the proton moves along the axis of zigzag (15,0)–zigzag (27,0) 2WCNT, at lower speeds $v = 0.6, 0.7, 0.8$ a.u. in (a) and (b), and higher speeds $v = 1.6, 1.7, 1.8$ a.u. in (c) and (d).

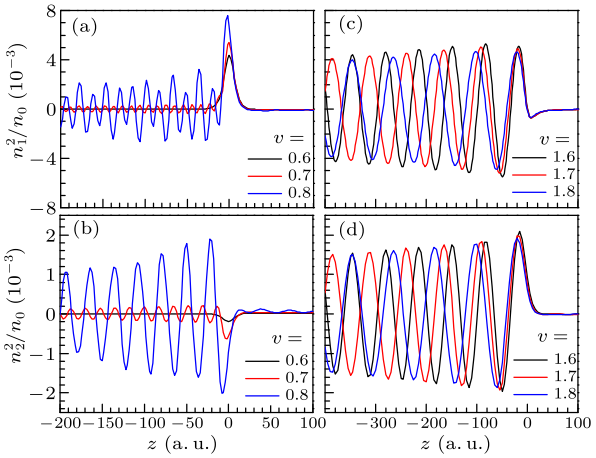

Fig. 3. Similar simulation results as those in Fig. 2, but in armchair (9,9)–armchair (15,15) 2WCNT.

For 2WCNTs, we show the rate of inner induced electron density $\frac{n_1^2}{n_0}$ and outer induced electron density $\frac{n_2^2}{n_0}$ versus axial direction z in the plane $\phi = \phi_0$ in Figs. 2 and 3. Here, two 2WCNTs are chosen: with inner zigzag (15,0) ($a_1 = 11.25$ a.u.) and outer zigzag (27,0) ($a_2 = 20.25$ a.u.) in Fig. 2, or inner armchair (9,9) ($a_1 = 11.69$ a.u.) and outer armchair (15,15) ($a_2 = 20.79$ a.u.) in Fig. 3. Dependencies of induced

electron densities $\frac{n_1^2}{n_0}$ and $\frac{n_2^2}{n_0}$ on the axial position z and the projectile speed are similar to those in SWCNTs. From Figs. 2(b) and 2(d), the valence electrons on the outer walls are largely excited by the inner polarized electrons which are induced by the incident particle. These excitations are stronger than those which are perturbed directly by the intruding particle without the inner walls, as shown in Figs. 1(a) and 1(b) in the zigzag (27,0) nanotube, leading to larger amplitude of the wake oscillation and smaller wavelength. Similar results can also be found on the outer wall of armchair (9,9)-armchair (15,15) nanotube shown in Figs. 3(b) and 3(d), compared with the results in armchair (15,15) nanotube in Figs. 1(c) and 1(d). Thus, it can be inferred that the incident ion would expose larger energy loss from the excitation of the outer nanotube than that without an inner wall. In fact, in our previous work,[23] we found that the energy the incident ion loses in a 2WCNT is much larger than that in the outer SWCNT, but smaller than that in the inner SWCNT, owing to the strong interference effects between the two walls in the 2WCNT.

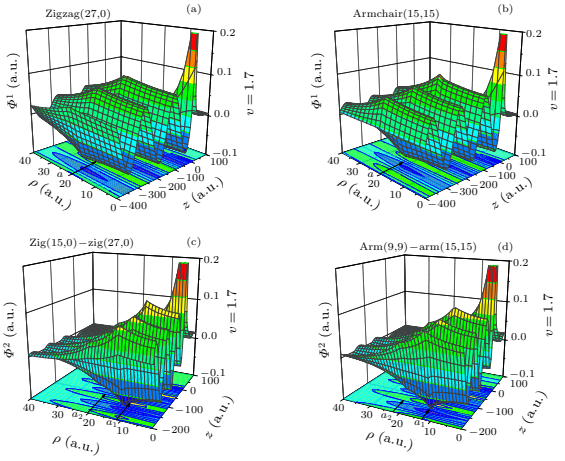

Fig. 4. Total potentials Φ^1 of SWCNT versus ρ and z positions for (a) zigzag (27,0) nanotube and (b) armchair (15,15) nanotube, and Φ^2 of 2WCNT for (c) zigzag (15,0)-zigzag (27,0) and (d) armchair (9,9)-armchair (15,15) nanotubes, induced by the proton moving along the axis of the nanotubes at fixed initial speed $v = 1.7$ a.u.

The 3D spatial variation of the total potential as the proton moves along the tube axis is shown in Fig. 4. Figures 4(a) and 4(b) display the total potential Φ_1^1 and Φ_2^1 inside and outside of zigzag (27,0) and armchair (15,15) nanotubes, respectively, at the fixed impact speed $v_0 = 1.7$ a.u. From the figures, there is a quite pronounced oscillation behind the particle along the z direction. Owing to the existence of the electron polarization induced by the proton, the oscillating wake potential exhibits a local extremum on the surface of nanotube wall ($\rho = a$), which becomes decaying significantly inside ($\rho < a$) and outside ($\rho > a$) nanotubes. The total potentials Φ^2 of 2WCNT for the proton moving along the axis of zigzag (15,0)-zigzag (27,0) nanotubes and armchair (9,9)-armchair (15,15) nanotubes at the same incident speed are also investigated, as shown in Figs. 4(c) and 4(d). Similar to the case in SWCNTs, local extrema around the inner and outer walls of nanotubes along the ρ direction are displayed, and the excitations of valence electrons on the outer walls induced by polarized electrons on the inner walls can be noticed clearly.

In summary, based on a semi-classical kinetic theory combined with the dielectric response theory, we have investigated wake effects in proton transport through SWCNTs and 2WCNTs. The analytical expressions of the induced electron density and spatial potential have been derived, while considering the real band-structure of electrons on the nanotubes surface. The simulation results show that the induced electron density strongly depends on the projectile speed. A wake-like oscillation can be found in the axial distribution as the projectile speed is set above a threshold speed value. In addition, corresponding to the features of the induced electron density on the surface of nanotubes, the induced potential behind the incident particle also presents oscillations not only along the axial direction but also in the lateral region. There appear local extrema located at the walls of SWCNT and 2WCNT. The kinetic model will be adopted in future studies of charged particle channeling in or between walls of the multiwalled nanotubes, especially with different nanotube chiral angle.

References

[1] Zhu Z Y, Zhu D Z, Lu R R, Xu Z J, Zhang W and Xia H H 2005 *Proc. SPIE* **5974** 597413
[2] Chai G, Heinrich H, Chow L and Schenkel T 2007 *Appl. Phys. Lett.* **91** 103101
[3] Liu H T, He J, Tang J Y, Liu H, Pang P, Cao D, Krstic P, Joseph S, Lindsay S and Nuckolls C 2010 *Science* **327** 64
[4] Wang Y N and Mišković Z L 2002 *Phys. Rev.* A **66** 042904
[5] Wang Y N and Mišković Z L 2004 *Phys. Rev.* A **69** 022901
[6] Mowbray D J, Chung S, Mišković Z L, Goodman F O and Wang Y N 2005 *Nucl. Instrum. Methods Phys. Res. Sect.* B **230** 142
[7] Mowbray D J, Mišković Z L, Goodman F O and Wang Y N 2004 *Phys. Lett.* A **329** 94
[8] Radović I, Borka D and Mišković Z L 2011 *Phys. Lett.* A **375** 3720
[9] Zamkov M, Woody N, Shan B, Chakraborty H S, Chang Z, Thumm U and Richard P 2004 *Phys. Rev. Lett.* **93** 156803
[10] Klimov V V and Letokhov V S 1996 *Phys. Lett.* A **222** 424
[11] Gevorgian L A, Ispirian K A and Ispirian R K 1998 *Nucl. Instrum. Methods Phys. Res. Sect.* B **145** 155
[12] Zhevago N K and Glebov V I 1998 *Phys. Lett.* A **250** 360
[13] Bellucci S, Biryukov V M and Cordelli A 2005 *Phys. Lett.* B **608** 53
[14] Krasheninnikov A V and Nordlund K 2005 *Nucl. Instrum. Methods Phys. Res. Sect.* B **228** 21
[15] Dedkov G V 2002 *Surf. Coat. Technol.* **158** 75
[16] Mišković Z L 2007 *Radiat. Eff. Defects Solids* **162** 185
[17] Arista N R 2001 *Phys. Rev.* A **64** 032901
[18] Arista N R 2001 *Nucl. Instrum. Methods Phys. Res. Sect.* B **182** 109
[19] Zhou D P, Wang Y N, Wei L and Mišković Z L 2005 *Phys. Rev.* A **72** 023202
[20] Slepyan G Ya, Maksimenko S A, Lakhtakia A, Yevtushenko O and Gusakov A V 1999 *Phys. Rev.* B **60** 17136
[21] Saito R, Fujita M, Dresselhaus G and Dresselhaus M S 1992 *Phys. Rev.* B **46** 1804
[22] Zhao D, Song Y H and Wang Y N 2008 *Chin. Phys. Lett.* **25** 2588
[23] Song Y H, Zhao D and Wang Y N 2008 *Phys. Rev.* A **78** 012901
[24] You S Y, Song Y H and Wang Y N 2009 *Nucl. Instrum. Methods Phys. Res. Sect.* B **267** 3133